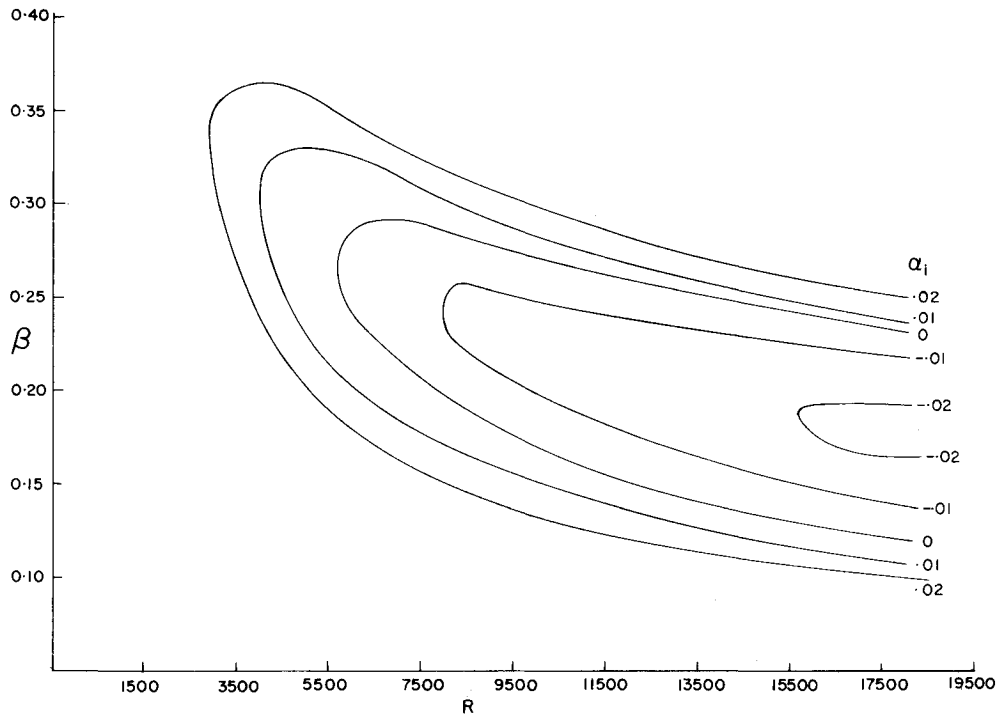

Fig. 3 Variation of β with R at constant α_i.

ranging from 1600 to 18,000. These results are plotted in Figs. 1 and 2 showing α_r and α_i vs the real frequency β. At each value of R the range of values of β was chosen to include the whole region of amplification and also sections of the damping region near the neutral curve. In Fig. 1, the graphs of α_r vs β are monotonically increasing and the slope of these lines, representing the reciprocal of the group velocity,[6] becomes slightly steeper as the Reynolds number increases. However, it is observed that at Reynolds number above 12,000, the slope $d\alpha_r/\partial\beta$, decreases with increasing β at values of β which correspond to points in the damping region beyond those of amplification. For amplification, α_i must be negative and it is evident from Fig. 2 that, according to the present calculations, the critical Reynolds number is slightly less than 6000.

The curves of α_i = const are shown in Fig. 3. The important parameters of the neutral stability curve are given in Table 1. The critical Reynolds number, according to present calculations, is 5778 and the corresponding value of α_r being 1.0219. The numerical calculations of Thomas[3] give a neutral stability curve which is almost identical with the present results. Thomas[3] found the critical Reynolds number to be 5780 with the corresponding α to be 1.026. Orszag's[7] results of the critical Reynolds number and wave number α were 5772 and 1.0206, respectively. His numerical solution was based on expressing the differential equations in terms of Chebyshev polynomials. The frequency β corresponding to the critical Reynolds number is found to be 0.269.

References

[1] Lin, C. C., "On the Stability of Two-Dimensional Parallel Flows," Pt. I–III, *Quarterly of Applied Mathematics*, Vol. 3, 1945, pp. 117–42, 218–34, 277–301.

[2] Shen, S. F., "Calculated Amplified Oscillations in Plane Poiseuille and Blasius Flows," *Journal of the Aeronautical Sciences*, Vol. 21, 1954, pp. 62–64.

[3] Thomas, L. H., "The Stability of Plane Poiseuille Flow," *Physical Review*, Vol. 91, 1953, pp. 780–783.

[4] Noumerov, B. V., "A Method of Extrapolating Perturbations," *Monthly Notices of the Royal Astronomical Society*, Vol. 84, 1924, pp. 592–606.

[5] Muller, D. E., "A Method for Solving Algebraic Equations using an Automatic Computer," *Mathematical Tables and Aids to Computation*, Vol. 10. No. 56, 1956, pp. 208–215.

[6] Gaster, M., "The Role of Spatially Growing Waves in the Theory of Hydrodynamic Stability," *Progress in Aeronautical Sciences*, 1st ed., Vol. 6, Pergamon, London, 1965, pp. 251–270.

[7] Orszag, S. A., "Accurate Solution of the Orr-Sommerfeld Stability Equation," *Journal of Fluid Mechanics*, Vol. 50, 1971, Pt. 4, pp. 689–703.

Experimental Study of Separation from the Base of a Cone at Supersonic Speeds

LYLE D. KAYSER*
U.S. Army Ballistic Research Laboratories, Aberdeen Proving Ground, Md.

AND

JAMES E. DANBERG†
University of Delaware, Newark, Del.

Introduction

FIGURE 1 qualitatively illustrates the nature of the base separation as observed in recent BRL Wind Tunnel tests on the base of a 10° half-angle sting supported cone. At the model corner, the external flow and the cone boundary layer expand through a strong expansion fan. The developing shear layer reattaches on the model sting support where part of the shear layer is recirculated back along the sting. This return flow separates from the sting close to the model and reattaches on the model base. Near the conical trailing edge, the recirculating flow separates again and merges with the shear layer downstream from the model. Apparently a small fraction of the cone surface boundary layer turns the corner and separates some distance from the corner along with the main recirculating flow.

Received May 6, 1974.

Index categories: Jets, Wakes, and Viscid-Inviscid Flow Interactions; Supersonic and Hypersonic Flow.

* Aerospace Engineer, Wind Tunnels Branch, EBL. Member AIAA.

† Professor, Department of Mechanical and Aerospace Engineering. Associate Fellow AIAA.

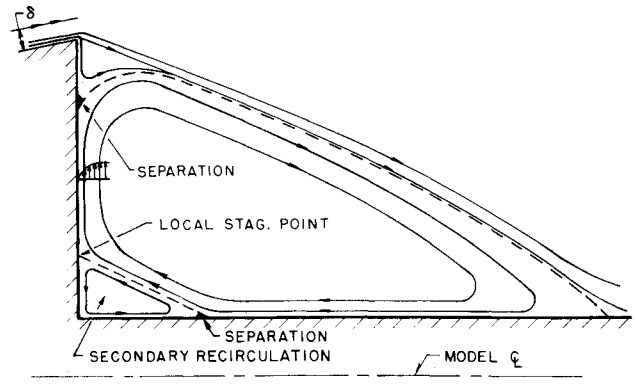

Fig. 1 Qualitative sketch of base separation phenomenon.

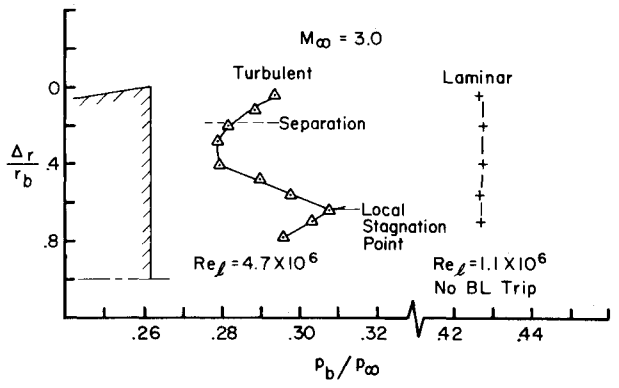

Fig. 3 Base pressure distribution.

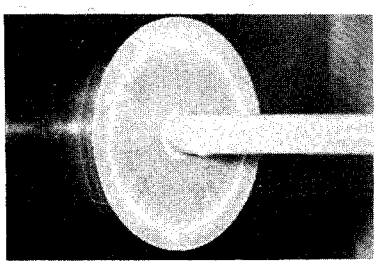

Fig. 2 Oil flow photograph, $M_\infty = 3.0$, $Re_l = 4.7 \times 10^6$.

Other investigators have observed or found evidence of base separation; however, conditions for which base separation occurs appear to vary widely. This Note briefly describes the conditions for which base separation was observed in the BRL tests. In these tests, a number of techniques were used to define in some detail the conditions under which base separation was observed.

Extensive base pressure measurements by Hama[1] over a 6° half-angle wedge for transitional flow were interpreted as indicating base separation. Donaldson[2] obtained pitot measurements aft of a trailing edge corner for both turbulent and laminar flows and reported that the shear layer appeared to originate on the base. For turbulent flow, Hong and Childs[3] reported observing separation on the base of a cylinder which was supported through the tunnel nozzle and hence had no sting. Shang and Korkegi[4] observed separation on the base of a step for laminar flow and local Mach numbers of 5.0–7.5. Small and Page[5] report that "The turbulent boundary layer when subject to favorable pressure gradients of expansion, has been observed to separate at the corner and undergo a reverse transition. In contrast, laminar boundary layers do not separate at the corner." Theoretical papers of Weinbaum[6] and Roache and Mueller[7] are attempts to correctly treat laminar flows near a corner without imposing restrictions on the position of separation. Weinbaum computed the flow near a sharp corner using a Stokes type series solution and shows that for the Stokes flow regime, flow can turn the corner and separate from a flat surface. Numerical solutions by Roache and Mueller showed that, for laminar flow, separation always occurred below the sharp corner with the distance from the corner decreasing with increasing Reynolds numbers; at $Re > 200$–300, distance of separation from the corner becomes very small.

Experiment

The tests were conducted on a 10° half-angle cone model at Mach 1.75–4.0. The model base diameter was 7.98 cm and the supporting sting was 1.35 cm in diameter. The experimental investigation was divided into the following four areas: 1) flow visualization tests which utilized shadowgraph, schlieren, and surface oil flow methods; 2) pressure measurements on the cone surface and base; 3) boundary-layer surveys on the cone surface; and 4) pitot pressure aft of the trailing edge corner. A more detailed description of the BRL experiment and results may be found in Ref. 8.

Results

The oil flow photograph of Fig. 2 clearly shows the oil accumulation ring on the cone base indicating separation; also, the oil accumulation on the sting indicates separation from the sting which causes the secondary circulation. The pressure distribution for turbulent flow shown in Fig. 3 is typical for the

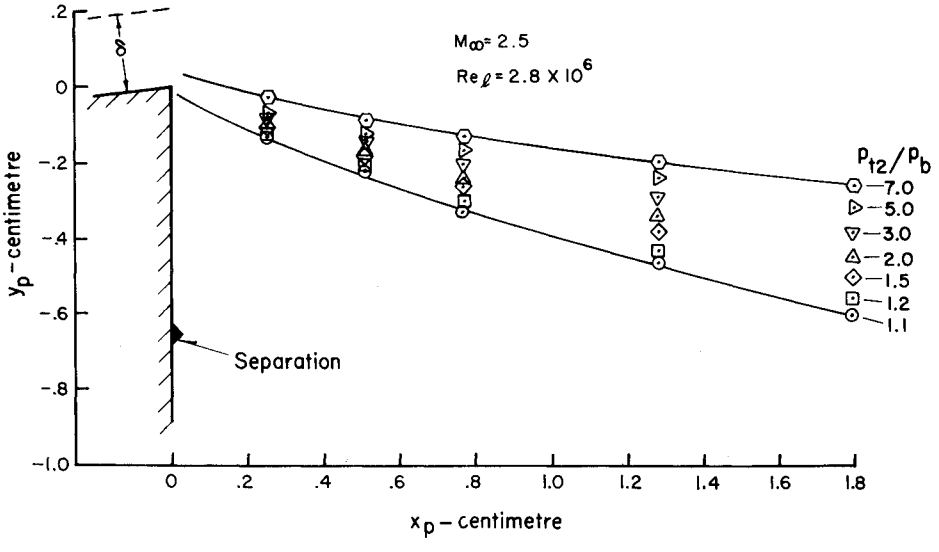

Fig. 4 Contours of constant impact pressure near the trailing edge corner.

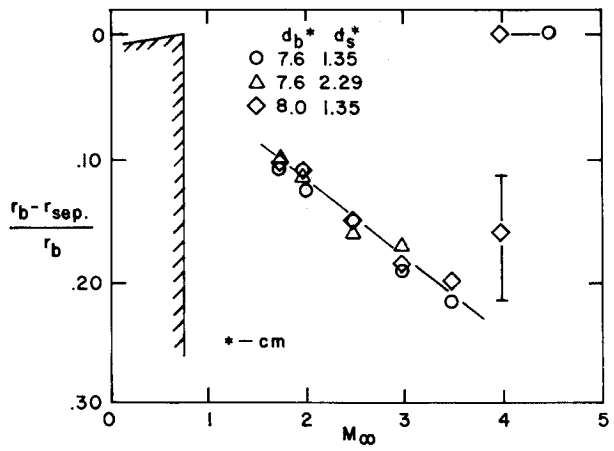

Fig. 5 Mach number effect on location of separation.

Mach number range of 1.75–3.5. Base separation always occurred between the trailing edge corner and the pressure minimum indicating that the radially outward recirculating flow encounters an adverse pressure gradient and then separates. The base pressure gradients near the corner are opposite in sign to those reported by Hama[1]; he interpreted his results as an overexpansion of the flow which turned the corner, encountered an adverse pressure gradient moving away from the corner, and then separated. BRL results at Mach 4.0 and 4.5 showed that base pressure gradients diminished and separation appeared to revert to the corner. For laminar flow, no significant pressure gradients were found to exist (Fig. 3) and oil flow tests indicated separation at the corner. Of the references cited, only the results of Hong and Childs[3] were qualitatively similar to the BRL results. Pitot traverses of Fig. 4 do not show evidence of the shear layer originating from the base; since the oil flow pictures clearly show a base separation, it is concluded that only a slight portion of the boundary-layer flow turns the corner. In contrast, Donaldson's pitot measurements indicate the origin of the separated shear layer is on the base.[2] Attempts at correlating parameters such as Reynolds number and boundary-layer thickness with position of separation were generally not successful; however, the position of separation did appear to be dependent on Mach number as seen in Fig. 5.

Conclusions

1) Separation occurred on the base for turbulent flow and the position of separation is dependent on Mach number. 2) Separation always occurred between the pressure minimum and the trailing edge corner. 3) Separation for laminar flow is at the corner or sufficiently near the corner that the distance cannot be detected by the oil flow method. 4) Theoretical predictions of base separation attribute such phenomena to laminar flows and predict stronger Reynolds number dependence than observed in the present tests.

References

[1] Hama, F. R., "Experimental Studies on the Lip Shock," *AIAA Journal*, Vol. 6, No. 2, Feb. 1966, pp. 212–219.

[2] Donaldson, I. S., "On the Separation of a Supersonic Flow at a Sharp Corner," *AIAA Journal*, Vol. 5, No. 6, June 1967, pp. 1086–1088.

[3] Hong, Y. S. and Childs, M. E., "Experimental Study of Axially-Symmetric Base Flow with Turbulent Initial Boundary Layer at $M_\infty = 2.42$," AIAA Paper 70-796, Los Angeles, Calif., 1970.

[4] Shang, J. S. and Korkegi, R. H., "Investigation of Flow Separation over a Rearward-Facing Step in a Hypersonic Stream," *AIAA Journal*, Vol. 6, No. 5, May 1968, pp. 986–987.

[5] Small, R. D. and Page, R. H., "Turbulent Supersonic Boundary Layer Flow in the Neighborhood of a 90° Corner," *Astronautica Acta*, Vol. 8, Pergamon Press, New York, 1973, pp. 99–117.

[6] Weinbaum, S., "On the Singular Points in the Laminar Two-Dimensional Near Wake Flow Field," *Journal of Fluid Mechanics*, Vol. 33, Pt. I, 1968, pp. 38–63.

[7] Roache, P. J. and Mueller, T. J., "Numerical Solutions of Laminar Separated Flows," *AIAA Journal*, Vol. 8, No. 3, March 1970, pp. 530–538.

[8] Kayser, L. D., "Experimental Study of Separation From the Base of a Cone at Supersonic Speeds," Masters Thesis, May 1974, Univ. of Delaware, Newark, Del.

Effect of Stress on the Directions of Stiffness Extrema

A. A. G. Cooper*
Babcock & Wilcox Company, Alliance, Ohio

Nomenclature

S_{ij}* = component of compliance tensor referred to x, y axes
U = $2x$ elastic energy stored in unit element
V_2, V_3 = see Appendix
p = $V_3(1-s)/[V_2(1+s)]$
s = σ_b/σ_a, $-1 \leqq s \leqq 1$
x, y = principal stress directions
θ = orientation of 1(2) axis with respect to $x(y)$ axis
σ_a, σ_b = principal stresses, $|\sigma_a| \geqq |\sigma_b|$
1, 2 = axes of material symmetry

Introduction

In some orthotropic materials the directions of maximum and minimum stiffness for a given state of stress depend not only on the elastic constants of the material but also on the applied stresses.[1,2]

This Note is a summary of an analysis of this behavior. The analysis is based on the use of stored elastic energy as a measure of stiffness. It is similar to but more detailed than the analysis given in Ref. 2 which resulted from the derivation of an optimality condition for reinforcement patterns in fiber reinforced composite structural components.

Analysis

Let a two-dimensional orthotropic unit element be subjected to a state of stress which is represented by its principal stresses σ_a and σ_b acting in the principal stress directions x and y, respectively. Let the 1 and 2 axes be the major and minor axis, respectively, of material symmetry. The orientation of the 1(2) axis with respect to the $x(y)$ axis is θ. The elastic properties are assumed to be the same in tension and compression.

The elastic stress energy stored in the unit element is adopted as a measure of the stiffness. With the stresses given, maximum (minimum) stiffness corresponds with minimum (maximum) elastic stress energy. (For a given uniaxial state of stress, stiffness and elastic stress energy are inversely proportional.)

The elastic stress energy stored in the unit element is given by

$$U/2 = \sigma_a{}^2[S_{11}{}^* + 2sS_{12}{}^* + s^2S_{22}{}^*]/2 \qquad (1)$$

To find the orientations for which the elastic energy attains an extremum, the first derivative of U with respect to θ is set equal to zero. The nature of the extremum is then determined from the sign of the second, third, and fourth derivatives at those values of θ for which the first derivative is zero.

From Eq. (1) and the transformation of S_{ij}* (see Appendix), the condition that the first derivative U' be zero gives

$$U' = -8\sigma_a{}^2 \sin(2\theta)[V_2(1-s^2) + V_3(1-s)^2 \cos(2\theta)] = 0 \qquad (2)$$

Received May 10, 1974; revision received June 24, 1974.
Index categories: Structural Composite Materials (Including Coatings); Structural Static Analysis.

* Project Engineer, Advanced Composites Department. Member AIAA.